at the nucleus by EPR for both divalent Mn^{55} and trivalent Fe^{57} are available for MgO [5,6] and ZnO [7,8] host crystals. In the case of MgO, the field for trivalent Fe^{57} is only about 5% lower in magnitude than the field for divalent Mn^{55}. In the case of ZnO, the field for trivalent Fe^{57} is about ten percent lower than that for divalent Mn^{55}. In spite of all of these complications, it is interesting to note that the field at the nucleus obtained by Mössbauer and EPR experiments are remarkably constant for various host crystals and for the isoelectronic ions divalent Mn^{55} and trivalent Fe^{57}.

The values of the field at the nucleus obtained by nuclear magnetic resonance have been reported recently by Boyd, Bruner, Budnick, and Blume[11] for various garnets and ferrites. They report two fields for magnetite of 460 and 490 koe magnitude in which the higher value is believed to correspond to the tetrahedral site which contains only Fe^{3+} ions.

Also, we note that the theoretical value of the field can be predicted from the spin-polarized Hartree-Fock calculations of Freeman and Watson[12,13] for free ions. In their treatment the s electrons are polarized by the $3d$ electrons. The difference in the electron spin density at the nucleus is conveniently given in terms of a function χ which has a value of -3.34 atomic units for Mn^{2+} and -3.00 atomic units for Fe^{3+}. These correspond to fields at the nucleus of -696 and -626 koe, respectively. This is considered to be very good agreement in view of the approximations involved in the calculations. In addition, the occurrence of covalent bonding and crystalline (Coulomb) field effects could reduce the magnitudes in solids compared to those of the free ion.

The Mössbauer results given here indicate that the field at the trivalent Fe^{57} nucleus in the spinel-type ferrites studied is the same to within a few percent at both the octahedral and tetrahedral sites. No changes in the Mössbauer spectrum can be observed between "ordered" and "disordered" crystals. It is not too surprising that no difference can be found between "ordered" and "disordered" crystals since the largest differences may be expected to be manifested in the quadrupolar interaction which is difficult to observe in powder ferrimagnetic samples. The magnitude of the field obtained by Mössbauer effect is in good agreement with that deduced from the hyperfine interaction parameter obtained from the electron paramagnetic resonance spectrum of the isoelectronic divalent Mn^{55} impurity in isomorphous crystals for both sets of sites.

ACKNOWLEDGMENTS

We should like to thank Dr. C. Cheek and Mr. E. Davis for preparing the source, Mrs. B. W. Henvis for assistance on calculations, and Mr. D. A. Gollnick for assistance in taking data. The sample of γ-Fe_2O_3 was kindly supplied by the Minnesota Mining and Manufacturing Company. We are grateful to Dr. F. J. Blatt, Dr. E. Prince, Dr. G. T. Rado, and Dr. A. J. Freeman for several helpful discussions.

PHYSICAL REVIEW VOLUME 124, NUMBER 1 OCTOBER 1, 1961

Diffusion of Zinc and Tin in Indium Antimonide*

SIMMON M. SZE† AND LING Y. WEI‡
Department of Electrical Engineering, University of Washington, Seattle, Washington
(Received December 19, 1960; revised manuscript received June 2, 1961)

The diffusion of zinc and tin in single-crystal and polycrystalline InSb has been studied with the radiotracer technique. The temperature dependence of the diffusion coefficients can be represented by: $D(\mathrm{Zn})=1.4\times10^{-7}\exp(-0.86/kT)$ cm²/sec and $D(\mathrm{Sn})=5.5\times10^{-8}\exp(-0.75/kT)$ cm²/sec in single-crystal InSb; and $D(\mathrm{Zn})=1.1\times10^{-6}\exp(-0.85/kT)$ cm²/sec in polycrystalline InSb, the activation energies being in electron volts. From the penetration curves, it appears that in polycrystalline InSb the zinc diffusion is a volume diffusion while the tin diffusion is mainly a grain boundary diffusion. The different behaviors of zinc and tin in InSb are discussed on the basis of one-type and two-type vacancy mechanisms.

INTRODUCTION

IN recent years, indium antimonide has been a subject of intense study. However, little has been reported on the solute diffusion in it. This is not without reason. Unless specially prepared, an InSb crystal used to contain undesired impurities of no less than 10^{14}/cc. For diffusion studies in this kind of crystal, the p-n junction method, which relies on conductivity measurements, would be less reliable. The radio-tracer technique, on the other hand, could produce dependable results if the half-life of the tracer as a diffusant is not too short compared with the diffusion time. Unfortunately, the time required for diffusion in InSb is relatively long (from several days to a few weeks). This would render experiment rather difficult if and when the

* This work was supported by the National Science Foundation.
† Present Address: Department of Electrical Engineering, Stanford University, Stanford, California.
‡ Present Address: Department of Electrical Engineering, University of Waterloo, Waterloo, Ontario, Canada.

short-lived tracers were used. Volatilization of the constituents and the diffusant from the surface during annealing further complicates the problem. From the above discussion, it is easy to understand why so little work has been done on the solute diffusion in InSb, the best known among III-V compounds.

In the present work, Zn^{65} and Sn^{115} have been diffused in InSb. These tracers were chosen because of their long half-lives (more than 100 days). Our purpose is to measure the diffusion coefficient and the activation energy for diffusion and also to investigate the specific mechanism involved in the diffusion. Since Zn is an acceptor and Sn may be either an acceptor or a donor in InSb, it would be interesting to see how they would behave in the InSb lattice. Both single-crystal and polycrystalline specimens were used so that the structure effect on diffusion could be examined.

EXPERIMENTAL

Single-crystal and polycrystalline InSb were obtained from Ohio Semiconductors, Inc. The single crystal has compensated impurities while polycrystals of both *n* and *p* types have impurity concentrations of 10^{18}/cc. Samples were cut to about 3 mm thickness with cross-sectional area 1.5 cm^2. They were first lapped and then ground in a precision grinding machine to be optically flat. The two faces of the specimen were parallel within 0.1 micron.

Radiotracers Sn^{113} (115 days half-life) and Zn^{65} (245 days) were procured from the Oak Ridge National Laboratory. The plating solutions were made as follows:

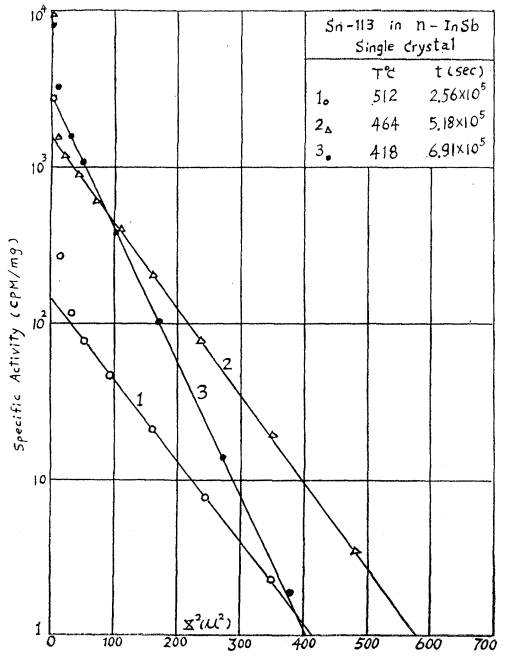

FIG. 1. Penetration curves of Sn diffusion in single-crystal InSb.

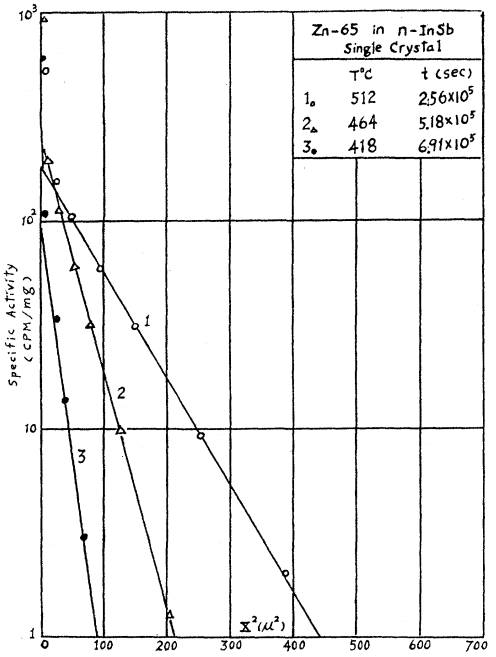

FIG. 2. Penetration curves of Zn diffusion in single-crystal InSb.

(1) Tin: $SnCl_2$ in HCl+50 ml H_2O+0.1 ml $NaHC_4H_4O_6$; (2) Zinc: $ZnCl_2$ in HCl+50 ml H_2O+ a few drops of concentrated HCl. After electroplating, the sample together with a quartz flat was put in a Pyrex tube. The tube was then evacuated to 10^{-3} mm Hg and thereafter filled with argon of 30 cm Hg. The pressure in the tube is to reduce the evaporation of the tracer from the surface of the specimen.

The samples were annealed for appropriate times ranging from 60 hr to 10 days, depending on temperature. A vertical-type furnace was used and the temperature was kept within 1°C over the annealing period. After cooling, the sample was taken out of the tube. The edges around the specimen were ground off to a depth of several diffusion lengths to remove the penetration by side diffusion. This was followed by sectioning, weighing, and counting. Each cut had an average thickness of 2–3 microns. The activity of the ground-off material was counted with end-window (TGC-3 Tracerlab tube) Geiger counter-scaler. We estimated the counting efficiency to be 20%.

RESULTS

1. Diffusion of Zinc and Tin in Single-Crystal InSb

Figures 1 and 2 show the penetration curves for the diffusion of Zn^{65} and Sn^{113} in single-crystal InSb. They fit very well the Gaussian function solution of Fick's law:

$$N(x,t)=S/(\pi Dt)^{\frac{1}{2}}\exp(-x^2/4Dt). \quad (1)$$

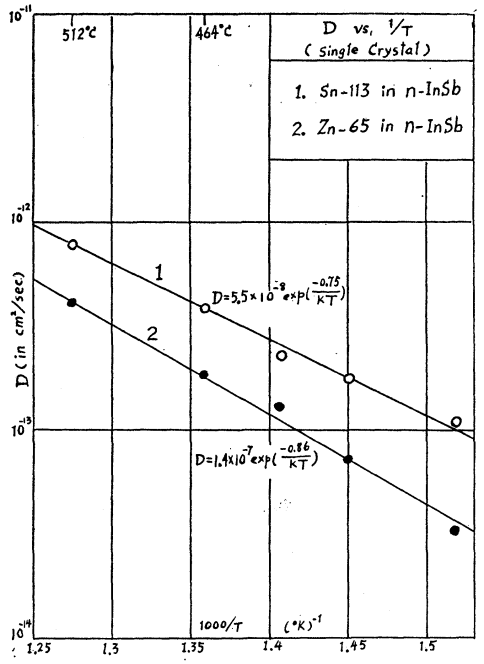

FIG. 3. Diffusivities of Sn and Zn vs the inverse temperature in single-crystal InSb.

This solution holds for the "limited source" condition at the surface. In Fig. 3 are shown the plots of the D vs $(1/T)$. They can be represented by:

$$D(\mathrm{Sn}) = 5.5\times10^{-8}\exp(-0.75/kT)\ \mathrm{cm^2/sec}, \quad (2)$$

$$D(\mathrm{Zn}) = 1.4\times10^{-7}\exp(-0.86/kT)\ \mathrm{cm^2/sec}, \quad (3)$$

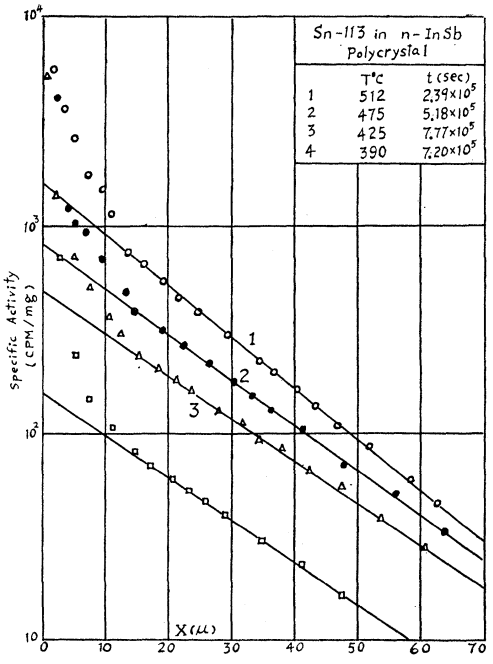

FIG. 4. Penetration curves of Sn diffusion in polycrystalline InSb.

TABLE I. Comparison of volume diffusion coefficients of tin in single-crystal and polycrystalline InSb.

Sample No.	T (°C)	t (sec)	D (cm²/sec) single crystal	D (cm²/sec) polycrystalline
1	512	2.29×10^5	7.9×10^{-13}	8.5×10^{-13}
2	475	5.18×10^5	4.5×10^{-13}	6.0×10^{-13}
3	425	7.77×10^5	2.0×10^{-13}	2.9×10^{-13}
4	390	7.20×10^5	1.1×10^{-13}	1.3×10^{-13}

where activation energies are in electron-volts. In the temperature range (400–512°C), D(Sn) is about twice D(Zn). The activation energies for diffusion are less than one electron volt.

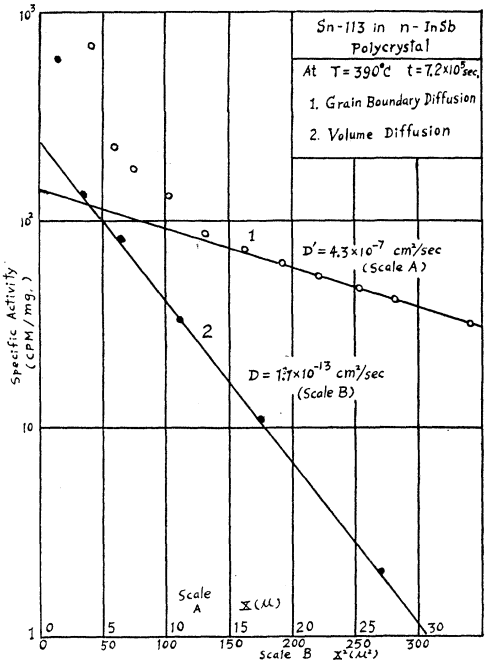

FIG. 5. Penetration curves of Sn diffusion (T=390°C) in polycrystalline InSb (n-type).

2. Diffusion of Tin in Polycrystalline InSb

As shown in Fig. 4, the logarithm of tin concentration in polycrystalline InSb varies linearly with the distance, characteristic of the grain boundary diffusion. Near the surface, volume diffusion may have comparable contribution to the solute concentration, thus making the curve nonlinear.

To separate the concentrations arising from the two different processes, we resorted to the method of analysis based on Fisher's paper.[1] The straight-line section of the curve is extended to the y axis. Let $y_1(x)$ and $y_2(x)$ represent the curved part and the extended straight line, respectively. Then the difference $\Delta y = y_1 - y_2$ may be taken as the activity resulting from the volume

[1] J. C. Fisher, J. Appl. Phys. 22, 74 (1951).

diffusion. In other words, they represented the tin atoms coming directly from the surface through the bulk. The corrected activities were then plotted against the square of the penetration. Such a plot gives a straight line as shown in Fig. 5 (curve 2). The diffusion coefficient calculated from this curve is very close to that of tin in single-crystal InSb, as shown in Table I.

The next step is to calculate the coefficient of grain boundary diffusion. Fisher's equation is used,[1] i.e.,

$$a \sim \exp\left(\frac{-(2D)^{\frac{1}{2}}x}{(\delta D')^{\frac{1}{2}}4(\pi Dt)^{\frac{1}{2}}}\right), \tag{4}$$

or

$$\ln a = (2D)^{\frac{1}{2}}x/4(\delta D' Dt)^{\frac{1}{2}} + \text{const}, \tag{5}$$

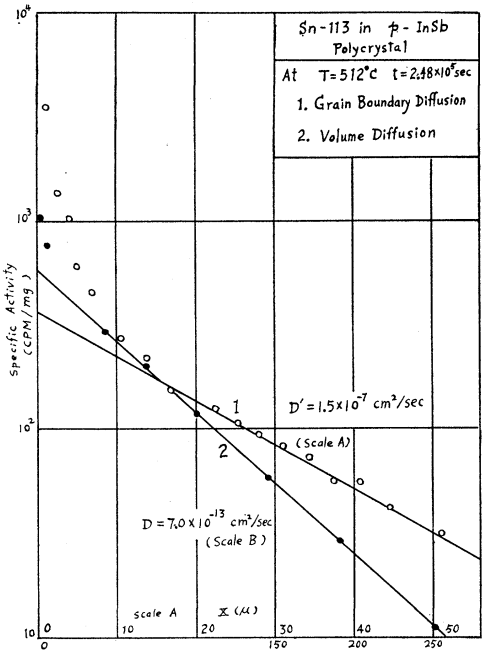

FIG. 6. Penetration curves of Sn diffusion (T=512°C) in polycrystalline InSb (p-type).

where a=the specific activity, D=the volume diffusion coefficient, D'=the grain boundary diffusion coefficient, and δ=the grain boundary thickness and is assumed to be about two atom layers (5×10^{-8} cm). With the aid of Eq. (5) and the values of volume diffusivity (D), it is possible to obtain D'. These are given in Table II.

Since the polycrystal we used has many grains of

TABLE II. Apparent grain boundary diffusivity of Sn^{113} in polycrystalline InSb (n-type).

Sample No.	T (°C)	D' (cm²/sec)	D (cm²/sec)	D'/D
1	512	1.27×10^{-7}	7.9×10^{-13}	1.6×10^{5}
2	475	7.2×10^{-8}	4.5×10^{-13}	1.6×10^{5}
3	425	1.9×10^{-8}	2×10^{-13}	1.0×10^{5}
4	390	4.3×10^{-8}	1.1×10^{-13}	3.9×10^{5}

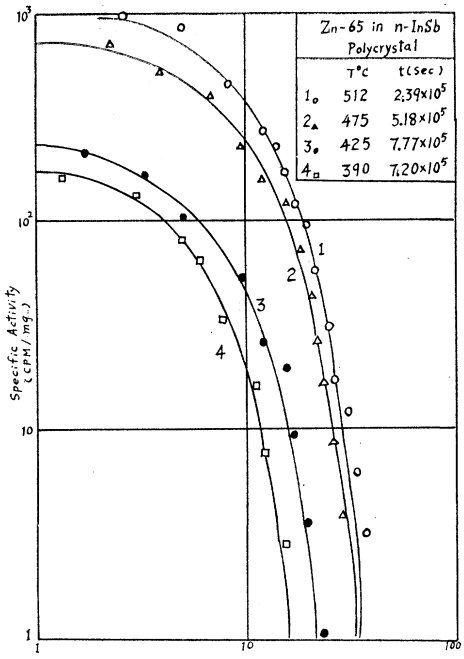

FIG. 7. Penetration curves of Zn diffusion in polycrystalline InSb (p-type).

polyhedral shape, the calculation based on Fisher's simple model is good only to give the order of magnitude of D' but not the activation energy.

A specimen of p-type polycrystalline InSb was annealed at 512°C for three days. As shown in Fig. 6, the penetration curve is similar to the curves shown in

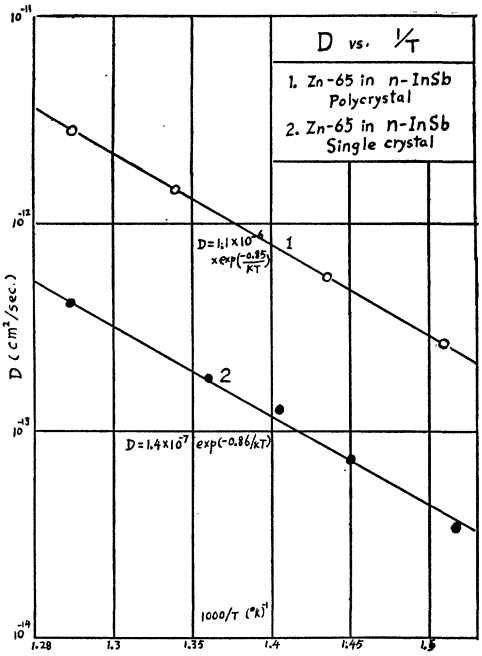

FIG. 8. Diffusivities of Zn vs the inverse temperature in InSb.

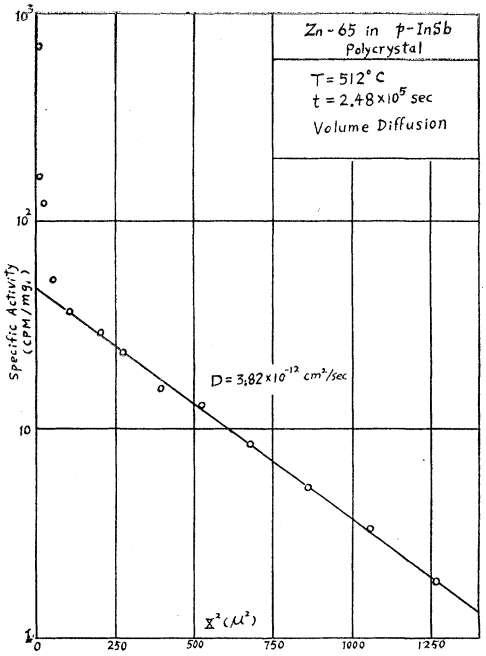

FIG. 9. Penetration curve of Zn diffusion in polycrystalline InSb (p-type).

Fig. 4. By the same procedure we found

$$D=7\times10^{-13}\ \text{cm}^2/\text{sec},$$
$$D'=1.5\times10^{-7}\ \text{cm}^2/\text{sec},$$

which were very close to the values of the diffusivities of tin in n-type polycrystalline InSb (see Table II).

3. Diffusion of Zinc in Polycrystalline InSb

As shown in Fig. 7, the concentration of Zn^{65} in polycrystalline InSb fits very well the erfc function solution of the Fick's law:

$$N(x,t)=N_0\ \text{erfc}[x/2(Dt)^{\frac{1}{2}}], \tag{6}$$

where N_0 is the concentration at the surface. The condition of "constant surface concentration" was believed to hold in this experiment because we deposited a very thick layer on the surface of the specimen. The temperature dependence of D is shown in Fig. 8, curve 1, which can be represented by

$$D=1.1\times10^{-6}\exp(-0.85/kT). \tag{7}$$

From Eqs. (3) and (7), we found that the activation energies for the diffusion of zinc in both single-crystal and polycrystalline InSb are essentially the same. The diffusion coefficient is increased by a factor of eight for diffusion in polycrystalline n-type InSb.

A specimen of p-type polycrystalline InSb was annealed at 512°C. Figure 9 shows the penetration curve of $\log N$ vs x^2. The diffusion coefficient calculated is $D=3.8\times10^{-12}$ cm²/sec, which is very close to that found in n-type polycrystalline InSb. (see Fig. 3).

The gross errors caused by sectioning, weighing, and counting may be estimated from the scatter of experimental points in the penetration curves. Based on Figs. 1 and 2, we estimated the errors in $C(x)$ to be no greater than $\pm15\%$.

Since the diffusion time was rather long (3–10 days), no corrections were made for the warm-up and cooling times (less than 10 min). The flatness and parallelism of the two faces of the specimen were checked and found to be within 0.1 micron. The maximum error in x^2 (from the second experimental point on) was estimated less than 1% and the maximum inclination of the finished face after 15 cuts with the original (uncut) face, less than 10^{-2}°.

The D value would be very different had evaporation of diffusant from the surface taken place. To prevent this, we filled the tube with argon at a pressure of 30 cm mercury. As a check, the surface activity was measured before and after diffusion and found to have no noticeable change. Thus we were assured that the diffusivity as obtained from this experiment was not complicated by the evaporation process.

From the above discussion, we estimated the error in D to be not over $\pm20\%$. The uncertainties in D_0 and Q (activation energy) may be estimated from the curves of D vs $1/T$. Based on Fig. 3, we get

$$\Delta Q=\pm5\%,\quad \Delta D_0=\pm50\%.$$

DISCUSSION

Self-diffusion in InSb had been studied by a number of workers.[2,3] Their results are in substantial disagreement. Hulme and Kemp[4] investigated Zn diffusion in InSb, and by the p-n junction method obtained $D_0=1.6\times10^6$ cm²/sec and $Q=2.3\pm0.3$ ev. The wide discrepancy in D_0 and Q obtained by various workers is perhaps due to the variance in the make of crystal and the technique of measurement used in the experiment. We might mention in passing that in Hulme and Kemp's experiment, the range of uncertainty of D measured was shown to be as high as 1:100. This is two orders of magnitude greater than usually found in tracer measurements.

Figure 8 shows that the diffusivity of Zn in a polycrystal is about eight times that in a single crystal. This indicates the structure effect. Some workers have already found that the diffusivity in a deformed crystal (bent, strained, or twisted) is higher (by 10 to 1000 times) than that in an undeformed crystal.[5,6,7] Ap-

[2] F. H. Eisen and C. E. Birchaenall, Acta Met. **5**, 265 (1957).
[3] B. J. Boltaks and G. S. Kulilov, Zhur. Tekh. Fiz. **27**, 82 (1957).
[4] K. F. Hulme and J. E. Kemp, J. Phys. Chem. Solids **10**, 335 (1959).
[5] C. S. Fuller and J. A. Ditzenberger, J. Appl. Phys. **28**, 40 (1957).
[6] Ia. S. Umanski *et al.*, *Physical Nature of Metals* (Metallurgy Press, U.S.S.R., 1955).
[7] C. H. Lee, American Institute of Mining and Metallurgical Engineers Meeting, February, 1958, New York (unpublished).

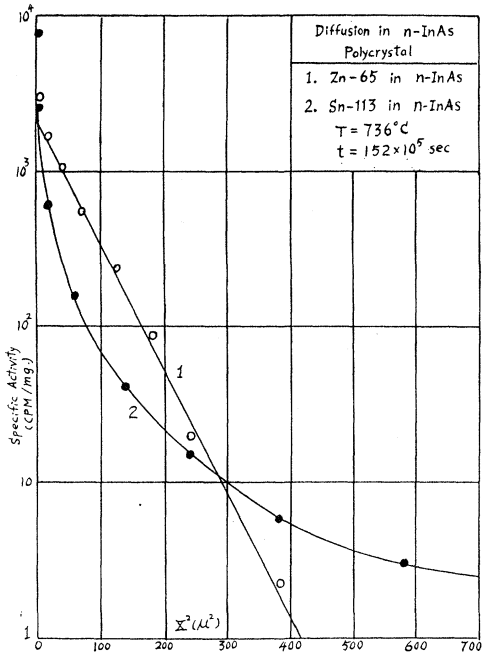

FIG. 10. Penetration curves of Zn and Sn diffusion in polycrystalline InAs.

ERRORS

parently, the structure defects (dislocations, grain boundaries, etc.) act as internal sources of vacancies which would enhance diffusion by the vacancy mechanism. The structure effect is also implied by the Zener's theory in which

$$D=\gamma a^2\nu \exp(\Delta S/k) \exp(-Q/kT).$$

In a more highly deformed crystal, the entropy ΔS could be larger and the activation energy (including the energy of vacancy formation) lower, and therefore the diffusivity (by a vacancy mechanism) would be higher than that in an undeformed crystal.

We shall now discuss the diffusion mechanism. From the previous work[2,8,9] it is generally believed that the self-diffusion and the solute (group II, IV, and VI elements) diffusion in III-V compounds are via vacancies within one, but not both, of the constituent sublattices. This may be called the one-type vacancy mechanism. One of the main purposes of this work was to see whether other mechanisms are also possible. From our work, we found that: (1) The activation energy for diffusion of tin in InSb is smaller than that of zinc. (2) The penetration curves (Figs. 4 and 7) indicate that the zinc diffusion in polycrystalline InSb is a volume diffusion while the tin diffusion is largely a grain boundary diffusion. To interpret both these facts, we suggested that the zinc diffusion is by a one-type (indium) vacancy mechanism but the tin diffusion is perhaps by a two-type (indium and antimony) vacancy mechanism. This proposition is based on the valency and the atomic size effects on diffusion. In valency, zinc is closer to indium than to antimony. On the other hand, tin falls between indium and antimony in both valency and atomic size. Thus, a tin atom would look upon the indium and antimony vacancies as alike, while a zinc atom would favor taking only an indium vacancy. In other words, an InSb crystal appears to be a more open structure for the diffusion of tin atoms than for that of zinc, and so the activation energy for the former would be smaller. This is just what we found in our experiment.

The different behaviors of Zn and Sn in polycrystalline InSb needs a little more exploration. It has been observed by others that during the growing of InSb crystal, the antimony atoms vaporize more rapidly than the indium atoms. It is not unreasonable to assume that the grain boundary in InSb is rich in antimony vacancies. If this is the case, the grain boundary would serve as an open channel to the tin atoms. The Sb-to-Sb jumps of tin atoms in the grain boundary would be much more frequent than those in the bulk of a single crystal. The zinc atoms, which could diffuse only via indium vacancies, would not see much benefit of the grain boundary and would behave in the same way in polycrystalline as in single-crystal InSb. Thus, in polycrystalline InSb, the Zn diffusion would be a volume diffusion while the tin would diffuse by a grain boundary mechanism.

W. S. Chen of our group has investigated Zn and Sn diffusion in polycrystal InAs at 736°C. The penetration curves are shown in Fig. 10. Here again the curve for the Zn diffusion is characteristic of volume diffusion, while that for the tin diffusion appears to represent a grain boundary diffusion. Schillmann's work on the diffusion in single-crystal InAs seemed to suggest that both Zn and Sn atoms diffuse via indium vacancies as they have the same activation energies. On the basis of resistivity and Hall measurements,[8] he believed that group IV elements enter the compound InAs with a replacement of indium atoms only. Though our work on diffusion in polycrystalline InAs was not extensive, the curves shown in Fig. 10 should provoke further thinking on the mechanisms of the Sn diffusion in InAs.

[8] E. Schillman, Z. Naturforsch **11a**, 463 (1956).
[9] B. Goldstein, Phys. Rev. **118**, 1025 (1960).